Future Vehicle driven by Electricity and Control
-Research on Four Wheel Motored "UOT Electric March II"-

Yoichi Hori
School of Engineering, Department of Electrical Engineering
University of Tokyo
7-3-1 Hongo, Bunkyo, Tokyo
113-8656 Japan
Phone: +81-3-5841-6678, Fax: +81-3-5841-8573
E-Mail: hori@hori.t.u-tokyo.ac.jp

Abstract

Electric vehicle is the most exciting object to apply "advanced motion control" technique. As an electric vehicle is driven by electric motors, it has following three remarkable advantages: (1) Motor torque generation is fast and accurate, (2) Motors can be installed in 2 or 4 wheels, and (3) Motor torque can be known precisely. These advantages enable us easily to realize (1) High performance ABS and TCS with minor feedback control at each wheel, (2) Chassis motion control like DYC, and, (3) Estimation of road surface condition. "UOT Electric March II" is our novel experimental EV with four in-wheel motors. This EV is made for intensive study of advanced motion control of electric vehicle, which can be firstly realized by electric vehicle.

Key words: Electric Vehicle, Motion Control, Adhesion Control, Slip Ratio Control, Antilock Braking System, Traction Control System, Direct Yaw Control, Estimation of Road Surface Condition, Body Slip Angle Estimation

1 Three Advantages of Electric Vehicle

Recent Pure Electric Vehicles (PEV) have already achieved enough driving performance thanks to drastic improvement of motors and batteries. On the otherhand, Hybrid EV's (HEV), like Toyota Prius, will be widely used in the next 10 years. Fuel Cell Vehicles (FCV) will be the major vehicles in the 21st century. As is well known, behind such development, strong incentive lies in energy efficiency and global environmental problem.

However, it is not well recognized that the most distinct advantage of electric vehicle is in the quick and precise torque generation of electric motor. If we do not utilize this merit, EV can never be used in the future. For example, if Diesel-HEV will be developed, its energy consumption can be extremely low. EV can not keep advantage against such vehicles in energy efficiency nor CO_2 emission. On the contrary, if we recognize the advantage of EV in control performance and succeed in development of new concept vehicles, bright future will be waiting for us.

We can summarize the advantage of EV into the following three points.

1. Torque generation of electric motor is very quick and accurate.
   This should be the essential advantage. Electric motor's torque response is several milliseconds which is 10-100 times as fast as that of the internal combustion engine or hydraulic braking system. This enables us feedback control and we can change vehicle characteristics without any change in characteristics from the driver. This is exactly based on the concept of Two-Degree-Of-Freedom(TDOF) control system. "Super ABS (Antilock Brake System)" will be possible. Moreover, ABS and TCS (traction control system) can be integrated, because a motor can generate both acceleration or deceleration torques. If we can use low drag tires, it will greatly contribute to energy saving.

2. Motor can be attached to each wheel.
   Small but powerful electric motors installed into each wheel can generate even the anti-directional torques on left and right wheels. Distributed motor location can enhance the performance of VSC (Vehicle Stability Control) such as DYC (Direct Yaw Control). It is not allowed for ICV (Internal Combustion engine Vehicle) to use four engines, but it is all right to use four small motors without so big cost increase.

3. Motor torque can be measured easily.
   There exists much smaller uncertainty in driving or braking torque generated by an electrical motor, compared to that of IC engine or

hydraulic brake. It can be known from the motor current. Therefore, simple "driving force observer" can be designed and we can easily estimate the driving and braking force between tire and road surface in a realtime manner. This advantage will contribute a great deal to application of new cotrol strategies based on road condition estimation. For example, it will be possible to give alarm to the driver "Now we have entered snowy road!"

These advantages of electric motor will open the new possibility of novel vehicle motion control for electric vehicles. Our final target is to realize a novel vehicle control system with four independently controlled in-wheel motors as depicted in Figs.1 and 2. It shows the integrated system with "minor feedback control loop at each wheel" and "total chassis controller" as outer weak feedback loop. Here, MFC (Model Following Control) is drawn as an example of the minor loop. Very short time delay is required for the actuator to perform such effective feedback controls.

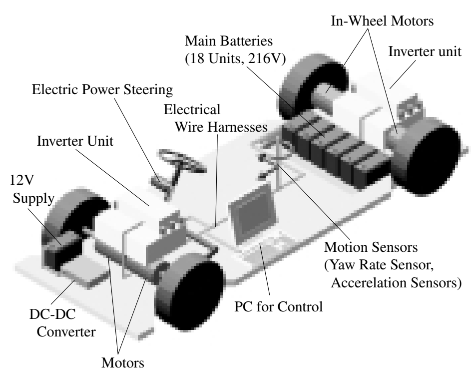

Fig. 1. Sketch to of "UOT March II".

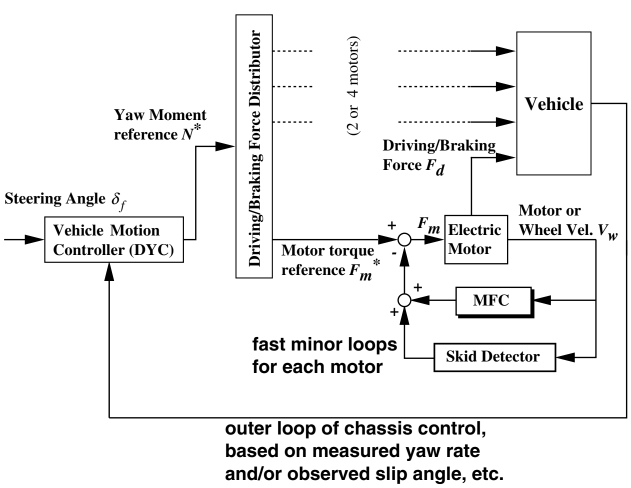

Fig. 2. Control system to be realized in "UOT March II".

2 What can we do with EV ?

As examples of novel control techniques, which can be realized firstly by EV, we are investigating a lot of techniques as follows. Due to the page limit, I would like to just list up our research topics.

2.1 Adhesion Control of Tire and Road Surface

In this type control methods, the advantage of an electric motor is most effectively utilized.

1. MFC (Model Following Control)
2. SRC (Slip Ratio Control)
3. Cooperation with higher level control like DYC
4. Wheel skid detection without vehicle speed

2.2 High Performance Braking Control

We can realize higher performance braking control system like an elevator utilizing electric motor's controllability.

1. Pure electric braking control in a whole speed range
2. Hybrid ABS for HEV. Fast but small torque electric brake can assist hydraulic brake system, which has big torque but slow response.
3. Direct control of driving force at each tire

2.3 Two-dimensional Attitude Control

The aim of two-dimensional attitude control is basically to find the solution to the problem how to mix the controls of γ (yaw rate) and β (body slip angle). It consists of linearization of transfer characteristic from driver's angle δ_f to γ and control β to be zero.

1. Decoupling control of β and γ
2. Higher performance AFS (Active Front Steering) and DYC
3. Vehicle dynamics control based on estimation of β
4. Dynamic driving force distribution considering side force
5. Driving force distribution considering cooperation with suspension system under changing load.

2.4 Road Surface Condition Estimation

As the motor torque can be known easily from the motor current, we can apply various kind of estimation techniques.

1. Estimation of gradient of $\mu - \lambda$ curve
2. Estimation of the maximum friction coefficient
3. Estimation of the optimal slip ratio to be used for SRC
4. Higher performance DYC based on the estimation of road surface condition

2.5 What is the Best Variable to be Given to/from the Vehicle?

This is an interesting discussion on what command the driver should give the vehicle. Is it torque command, speed command or something between them? What information from the vehicle is useful for the driver? In EV, any choice is OK by sophisticated control technique.

2.6 Electric Power Steering

EPS (Electric Power Steering) system is the best device to give the driver the vehicle condition in a real time manner. This viewpoint should be emphasized more.

3 Novel Experimental Electric Vehicle "UOT March II"

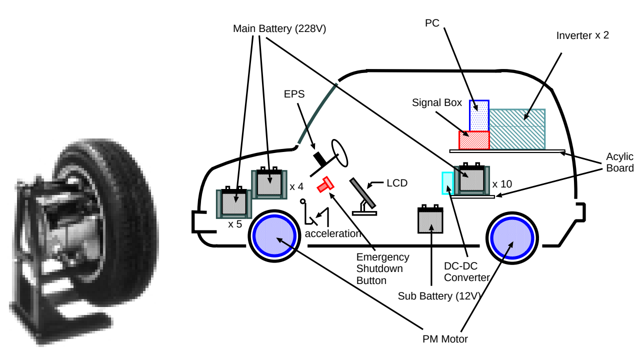

Fig. 3. In-wheel motor / Configuration of "UOT Electric March II".

Our new EV "UOT (University of Tokyo) Electric March II" is constructed in 2001 to perform experiments on novel control techniques. The most remarkable feature of this EV is that an in-wheel motor is mounted in each wheel. We can control each wheel torque completely independently. Regenerative braking is of course available. We built this EV by ourselves by remodeling Nissan March.

Table. 1. Specifications of "UOT Electric March II".

Drivetrain	**4 PM Motors / Meidensya Co.**
Max. Power(20 sec.)	36 [kW] (48.3[HP])*
Max. Torque	77* [Nm]
Gear Ratio	5.0
Battery	**Lead Acid**
Weight	14.0 [kg](for 1 unit)
Total Voltage	228 [V] (with 19 units)
Base Chassis	**Nissan March K11**
Wheel Base	2360 [m]
Wheel Tread F/R	1365/1325 [m]
Total Weight	1400 [kg]
Wheel Inertia**	8.2 [kg]***
Wheel Radius	0.28 [m]
Controller	
CPU	MMX Pentium 233[MHz]
Rotary Encoder	3600 [ppr]***
Gyro Sensor	Fiber Optical Type

* ... for only one motor. ** ... mass equivalent.
*** ... affected by gear ratio.

Table 1 is the summary of the specification of "UOT March II". Four in-wheel motors drive the car shown in Fig.3. It uses PM motor and has in-built drum brake and reduction gear. The motor unit is as compact as the wheel. Two motors are placed at the ends of each driving shaft, and attached to the base chassis shown in Figs.4-7. The electric motors are controlled by on-board personal computers (PC's).

We use one more PC for motion control. They are connected to several sensors, for example, fiber-optical gyro sensor, three axis acceleration sensor and so on. Motion controller is installed in the second PC. It outputs the motor torque references, and two inverter units generate the required motor torques. Precise torque generation is achieved by the motor current controller in the inverter units. In order to detect steering angle, the encoder signal for EPS is used.

4 Antiskid Control in Longitudinal Direction

In this section, the wheel controller for skid prevention is proposed. The starting point of this idea is to utilize the knowledge obtained in advanced motion control techniques of electric motors. Generally speaking, feedback controller can change mechanical plant dynamics. For example, the plant can be insensitive against disturbance if an appropriate feedback controller is applied. Fast response of actuator, which is firstly available in EV, can realize such controls. We propose two anti-slip controllers: MFC (Model Following Control) and SRC (Slip Ratio Control).

Fig. 4. Front Motors

Fig. 5. Rear Motors

Fig. 6. Inverters

Fig. 7. Batteries

4.1 Model Following Control (MFC)

In the simple model of one wheel shown in Fig.8, the slip ratio λ is given by,

$$\lambda = \frac{V_w - V}{\max(V_w, V)} \tag{1}$$

where V is the vehicle chassis velocity, and V_w is the wheel velocity given by $V_w = r\omega$. r and ω are the wheel radius and rotational velocity, respectively.

Fig.9 shows the block diagram of Model Following Control (MFC). F_m is the acceleration command roughly proportional to the acceleration pedal angle. $F_m = Tr$, where T is the driver's command torque. ω increases drastically when the tire slips.

Vehicle dynamics including tire and road surface characteristics are very complicated, but if we use the slip ratio λ, the vehicle body can be seen as one inertia system with the equivalent inertia moment given by

$$M_{actual} = M_w + M(1 - \lambda) \tag{2}$$

Here, M_{actual}, M_w and M are the total equivalent mass, wheel mass and equivalent vehicle mass. (2) means that the vehicle seems lighter when the tire slips and λ increases. We used the following mass with $\lambda = 0$ as the reference model.

$$M_{model} = M_w + M \tag{3}$$

When there is no slip, actual M_{actual} is almost equal to M_{model}. No control signal is generated from MFC controller. If the tire slips, actual speed ω increases quickly. Model speed does not increase. Hence by feeding back the speed difference to motor current command, the motor torque is reduced quickly and it induces re-adhesion.

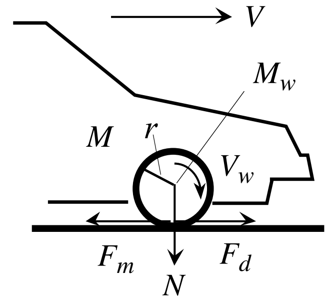

Fig. 8. One wheel model.

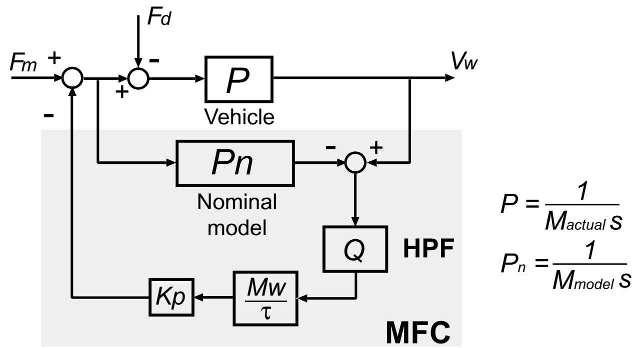

Fig. 9. Block diagram of the proposed feedback controller "MFC".

As this control function is needed only in relatively higher frequency region, a high pass filter with time constant τ is used on the feedback path.

When a vehicle starts skidding, the wheel velocity changes rapidly. For example, if vehicle starts skidding during acceleration, its wheel velocity increases rapidly, and during deceleration, it decreases rapidly due to the wheel lock. Such rapid change of wheel velocity is observed as a sudden drop of wheel inertia moment. Based on this viewpoint, we design the MFC as shown in Fig.9. Using (3) as the nominal model inertia, this controller can suppress sudden drop of inertia. Applying this controller, the dynamics of the skidding wheel becomes closer to that of the adhesive wheel.

Experiments were carried out with "UOT March-I", which is our first laboratory-made EV constructed in 1997. To examine the effect of MFC, slippery low μ road is required. We put the aluminum plates of 14[m] length on the asphalt, and spread water on these plates. The peak of this test road was estimated about 0.5.

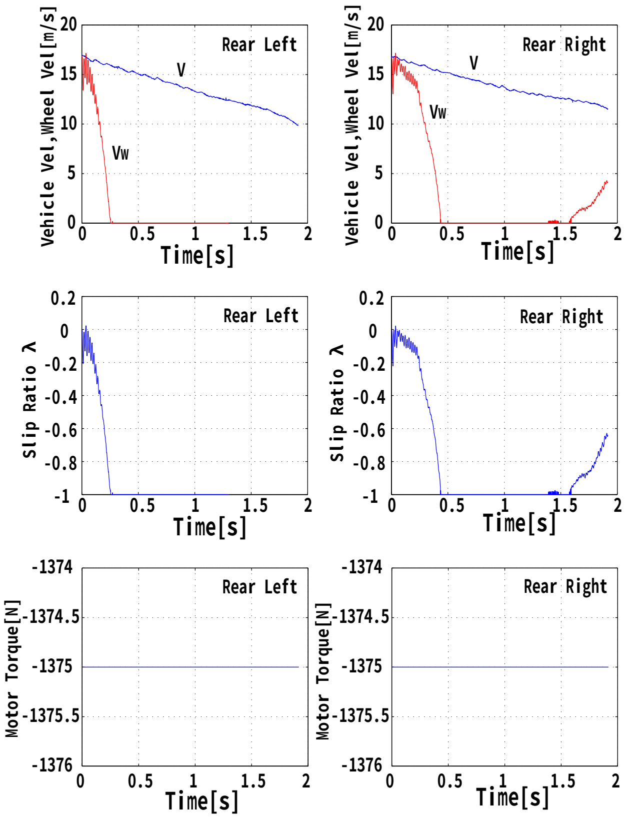

Fig. 10. Wheel lock in rapid braking “without MFC”.

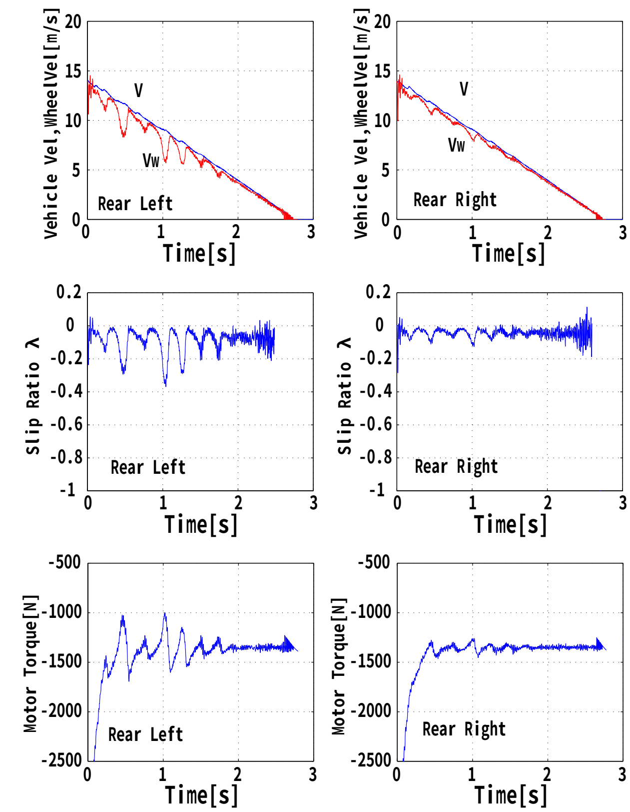

Fig. 11. Stable braking with our proposed controller “MFC”.

Fig.12 shows the time responses of slip ratio. In these experiments, vehicle was accelerated on the slippery test road, while the motor torque was increased linearly. Without control, the slip ratio rapidly increases. On the contrary, the increase of slip ratio is suppressed when the proposed controller is applied. Also, Figs.10 and 11 show the experimental results using “UOT March II” on a professional test course. It is decelerated suddenly on the slippery course, where μ_{peak} of the road was about 0.5. Without control, the wheel velocity was rapidly decreased and the vehicle’s wheels were soon locked as seen in Fig.10. In contrast to this, when MFC is applied, the change of wheel velocity is much smaller (Fig.11). The wheels were not locked, and the vehicle stopped safely.

Note that this method is not a complete skid prevention controller by itself. Rapid growth of slip ratio is suppressed, however, the slip ratio finally exceeded the stable limit (Fig.12). Therefore, we suggest this method can be used as a minor-loop controller just to assist other methods like conventional ABS or other skid detection techniques.

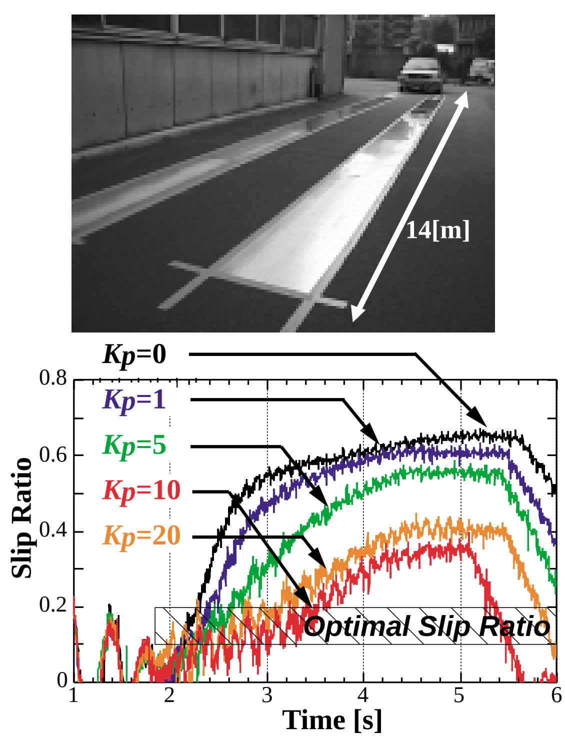

Fig. 12. Experimental results of MFC for skid prevention with $\tau = 0.1$.

Fig. 13. Braking experiment of "UOT Electric March II".

4.2 Slip Ratio Control (SRC)

MFC showed that the electric motor control can affect the mechanical characteristics. If we want more exactly to regulate the slip ratio within a specified range, more precise approach is necessary.

Based on the tire model shown in Fig.8, under some practical assumptions, the kinetic equations of the wheel and vehicle take the forms of

$$(F_m - F_d)\frac{1}{M_w s} = V_w \quad (4)$$

$$F_d \frac{1}{Ms} = V \quad (5)$$

The friction force between the road and wheel is given by

$$F_d = N\mu(\lambda) \quad (6)$$

where, F_m is the motor torque (force equivalent), F_d the friction force, M_w the wheel inertia (mass equivalent), M the vehicle weight, and N the vertical force given by $N = Mg$.

From (1), when $V_w >> V$, the perturbation system is given by

$$\begin{aligned}\Delta\lambda &= \frac{\partial\lambda}{\partial V}\Delta V + \frac{\partial\lambda}{\partial V_w}\Delta V_w \\ &= -\frac{1}{V_{w0}}\Delta V + \frac{V_0}{V_{w0}^2}\Delta V_w \quad (7)\end{aligned}$$

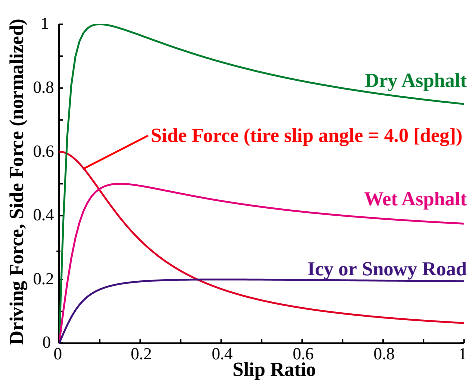

Fig. 14. Typical $\mu - \lambda$ curve.

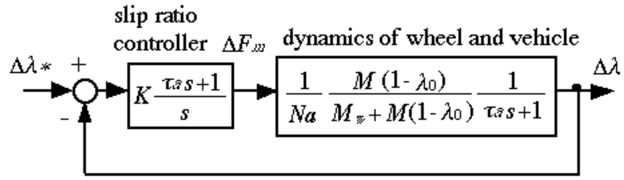

Fig. 15. Slip ratio controller (SRC).

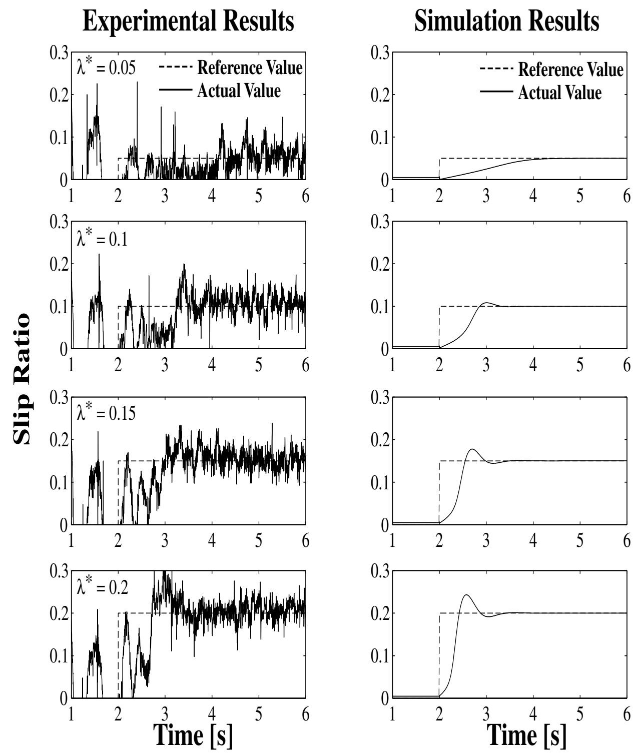

Fig. 16. Experimental results of SRC.

where V_{w0} and V_0 are the wheel and vehicle speeds at a certain operational point. The friction force is given by using a, the gradient of $\mu - \lambda$ curve. a is defined by

$$\Delta\mu = a\Delta\lambda \quad (8)$$

The transfer function from motor torque to slip ratio is obtained by

$$\frac{\Delta\lambda}{\Delta F_m} = \frac{1}{Na}\frac{M(1-\lambda_0)}{M_w + M(1-\lambda_0)}\frac{1}{\tau_a s + 1} \quad (9)$$

The time constant τ_a is given by (10), which is proportional to the wheel speed V_{w0}.

$$\tau_a = \frac{1}{Na}\frac{MM_w V_{w0}}{M_w + M(1-\lambda_0)} \quad (10)$$

The typical value of τ_a is 150∼200[ms] when $a = 1$ and the vehicle speed is around 10[km/h]. a can be negative in the right-hand side of the peak of $\mu - \lambda$ curve.

A simple PI controller with a variable proportional gain is enough as the slip ratio controller. It is given by (11) and drawn in Fig.15.

$$K\frac{\tau_a s+1}{s} \tag{11}$$

The transfer function from the slip ratio command to the actual slip ratio becomes

$$\frac{\Delta\lambda}{\Delta\lambda^*} = \frac{1}{1+Na\frac{M_w+M(1-\lambda_0)}{M(1-\lambda_0)}\frac{1}{K}s} \tag{12}$$

If $\lambda_0 << 1$, this is a simple first order delay system with the time constant to be adjusted by K. Here, we put this response time 50∼100[ms].

Fig.16 shows the experimental results of SRC using “UOT March I” and corresponding simulations. Here the target slip ratio is changed stepwise from 0 to various values from 0.05 to 0.2. We can see good performances in any cases.

5 Lateral Motion Stabilization

5.1 Vehicle Behavior Simulation with MFC in Each Wheel

In the previous section, the minor feedback control at each wheel was discussed. Next, our interest is in what will happen if we apply such feedback control to every wheel when the vehicle is turning on slippery road.

As is commonly known, the vehicle lateral motion can be sometimes unstable at rapid braking when the vehicle is cornering, in particular on a slippery road condition with snowy or rainy weather.

Here we assume that one in-wheel motor is independently attached on every wheel, and MFC is applied to each of them. The simulation results (Fig.17) show that this minor loop can enhance the lateral stability effectively. In simulations, chassis's 3-DOF nonlinear motion dynamics, four wheel's rotation and dynamic load distribution are also carefully considered.

The vehicle starts running on the slippery road where μ_{peak}=0.5, turning left with steering angle δ_f = 3[deg]. Then at t=5.0[sec], the driver inputs rapid braking torque F_m = -1100[N] on each wheel. This torque exceeds the limit of adhesion performance. Therefore, the wheel skid occurs and the chassis starts to spin, although the driver stops braking at t = 9.0[s]. This wheel skidding is serious in particular at rear-left wheel, since the center-of-gravity is shifted and the load distribution changed.

On the contrary, if MFC is applied independently for each wheel, such dangerous spin motion is prevented. The rear-left wheel's torque is reduced automatically. This method MFC uses only the local wheel velocity as the feedback signal in each wheel. Therefore, it differs from conventional attitude control methods like DYC. The autonomous stabilization of lateral motion is achieved only by minor feedback control at each wheel.

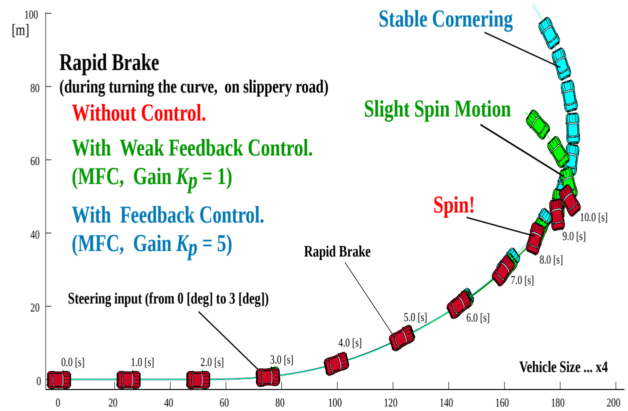

Fig. 17. Stabilizing effect with controlled four wheels is visualized with vehicle trajectory.

5.2 Experiments of Stability Improvement by MFC

Next, we performed actual experiments using ”UOT Electric March II”. In these experiments, ”UOT March II” turned on a slippery road, known as the skid pad. The rear-wheel velocities are controlled independently by the two rear motors, though ”UOT March II” has totally four motors.

At first ”UOT March II” was turning normally in the clock wise direction. The turning radius is about 25-30[m] and chassis velocity is about 40[km/h]. These values are close to those of unstable region. In these experiments, acceleration torque of 1000[N] was applied to the two rear motors. Without MFC, this rapid acceleration torque causes instability as shown in Fig.18. The rear right wheel began skidding with much danger. Then the yaw rate grew into unstable region. The vehicle was in spin motion and completely out of control. On the contrary, as is shown in Fig.19, such dangerous vehicle motion could not be observed. Fig.20 shows this effect more clearly.

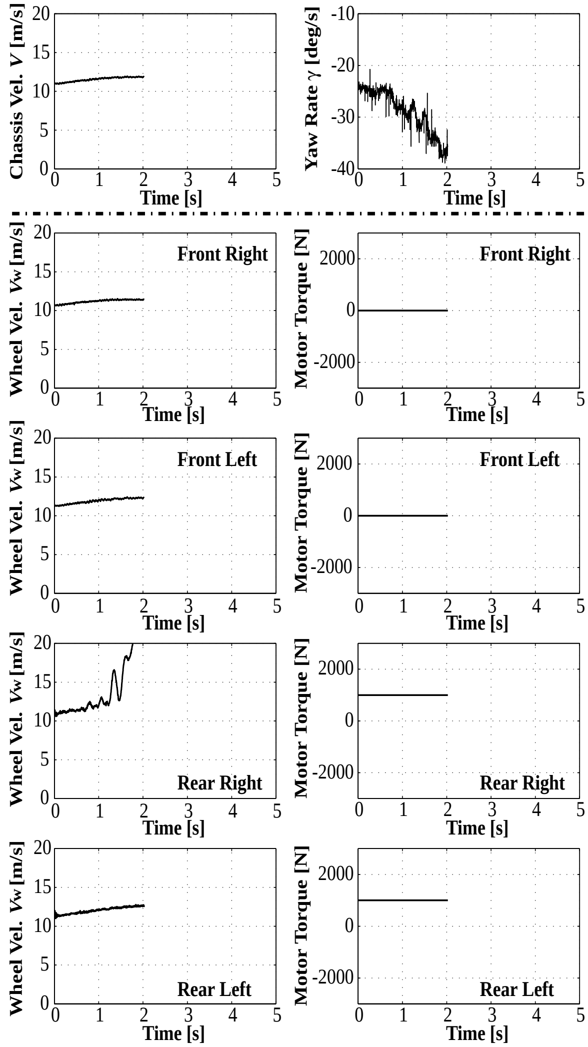

Fig. 18. Unstable cornering with sudden acceleration without MFC.

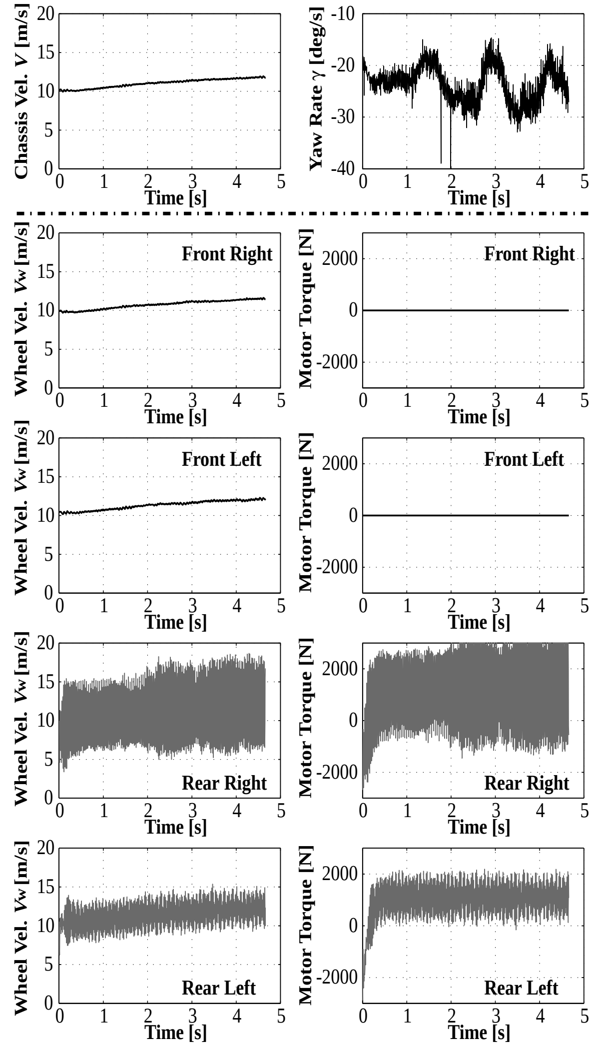

Fig. 19. Vehicle stabilizing effect of our proposed controller MFC.

Fig.21 shows a comparison of the vehicle's trajectories. It shows that the MFC controller prevents spin out caused by excessive over steer. In this case, the controllers on rear-right and rear-left are the same but independent from each other, but vehicle stability is still kept. In other words, autonomous stabilization of each driven wheel was achieved, and vehicle lateral stability was enhanced as well as the conventional DYC realizes. One of the remaining problems is the high-frequency oscillation in rear wheel torques. It appears in Figs.19 and 20. It is probably due to the improper design of the controller parameters. We will solve this problem in our next experiment.

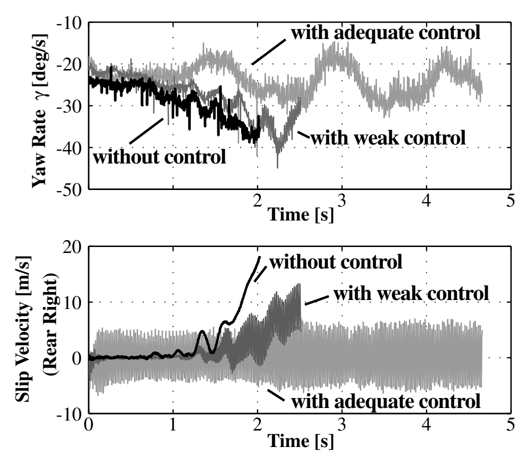

Fig. 20. Comparison of vehicle motion observed in γ and the slip velocity.

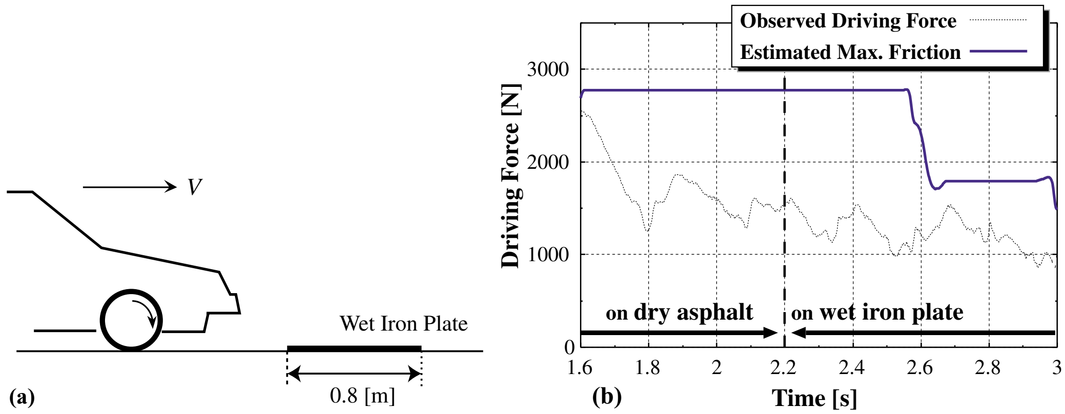

Fig. 22. Experimental results of road condition estimator.
The sudden road condition change (a) was sensed with estimated maximum friction force as shown in (b).

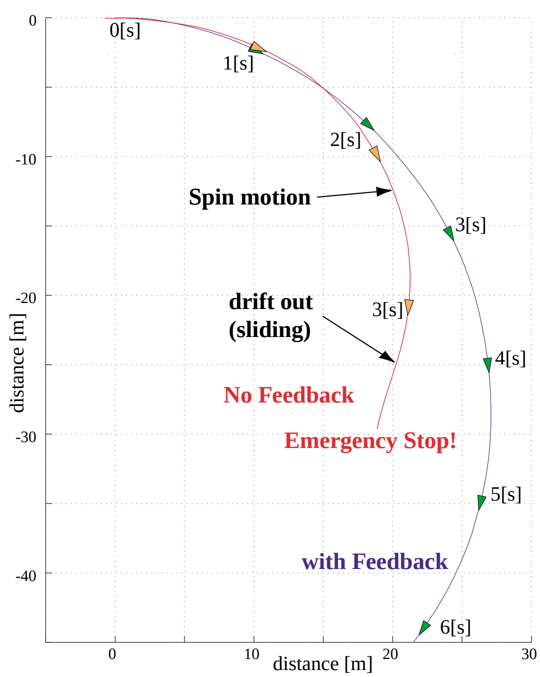

Fig. 21. Stabilizing effect of MFC installed in each wheel.

6 Estimation of Vehicle System Variables

As the motor torque can be generated precisely, accurate value of motor torque can be utilized as an important information for system parameter estimation. Estimation techniques are also important, because some important values like slip ratio λ, body slip angle β or road peak μ cannot be measured with practical sensors. These values should be estimated, if necessary. Such estimation can be firstly realized by using accurate motor torque value. In this section, three examples of such applications are introduced.

6.1 Road Condition Estimation

The road surface condition is the quite useful information for motion control. As this information will enhance the performance of ABS and DYC, therefore, road condition estimation is intensively studied also for conventional vehicles.

The accurate value of wheel input torque will contribute a great deal to the the practical and precise estimation. It is available on EV with electric motor, but not so easy on ICV with combustion engine. We have proposed advanced road condition estimator for EV, which estimates the peak value or maximum friction force during adhesive driving.

Fig.22 shows the typical experimental results with UOT March I. This EV runs on the dry asphalt road, then reaches the wet iron plate. The road condition estimator calculates the maximum friction force between tire and road surface. This value indicates the sudden change of road condition, as shown in the figure. Note that even if the actual driving force is always less than maximum frictional force, this method can estimate maximum friction force.

This technique can be used as the alarm system to tell the driver “Please be careful. Now the car has entered slippery road!”

6.2 Wheel Skid Detection without Vehicle Speed

Wheel skid detection is another application of accurate torque generation of electric motor. This method can detect the wheel skid without chassis speed measurement. As the motor torque F_m is known, driving force observer can be designed to estimate the driving force F_d, which is the friction

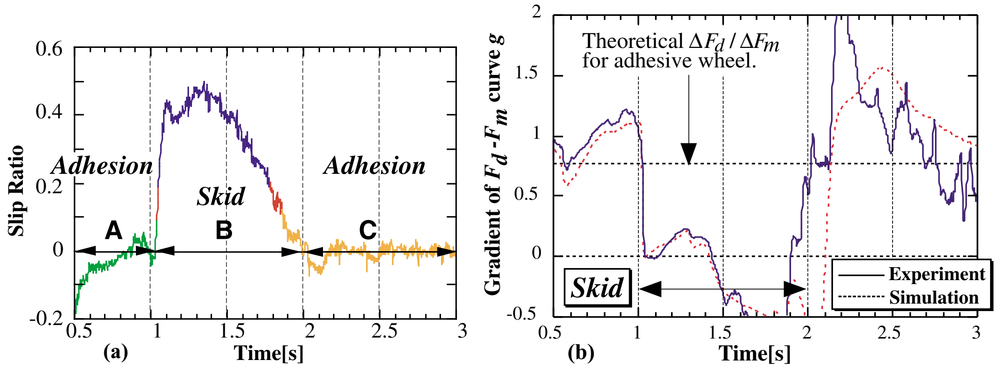

Fig. 23. Experimental results of wheel skid detector.
(a) Reference slip ratio indicates the serious skid occurred during 1-2[s], and (b) The proposed method detected it.

force between the road and tire. Its principle is same to disturbance observer. The skid detection algorithm is very simple. When F_m increases and F_d also increases, tire should be adhesive. When F_m increases but F_d dose not increases, then it is skidding. Fig.23 shows the experimental results using UOT March I, where we can see the validity of this method.

6.3 Estimation of Body Slip Angle β

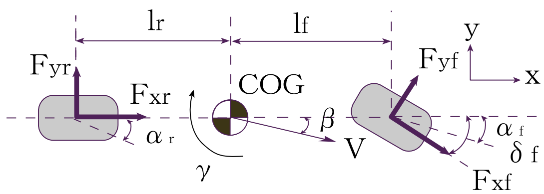

Fig. 24. Two wheel vehicle model.

Vehicle's body slip angle β increases in a dangerous driving situation and should be controlled to smaller value, but we need expensive optical sensors to measure it. We then propose the β observer. We expect it is robust to the model variation and works well even in non-linear region of vehicle motion.

Fig.24 shows the two wheel vehicle model, which is often used for vehicle motion analysis and controller design. Its state equations of are given by

$$\dot{\boldsymbol{x}} = \boldsymbol{A}\boldsymbol{x} + \boldsymbol{B}u \tag{13}$$

where

$$\begin{aligned}
\boldsymbol{x} &= (\beta \quad \gamma)^T, \quad u = \delta_f \\
\boldsymbol{A} &= \begin{pmatrix} \frac{-2(C_f+C_r)}{mV} & \frac{-2(C_f l_f - C_r l_r)}{mV^2} - 1 \\ \frac{-2(C_f l_f - C_r l_r)}{I} & \frac{-2(C_f {l_f}^2 + C_r {l_r}^2)}{IV} \end{pmatrix} \\
\boldsymbol{B} &= (\frac{2C_f}{mV} \quad \frac{2C_f l_f}{I})^T
\end{aligned}$$

In designing the β observer, the yaw rate γ has been used as the only measurable signal, but this conventional observer doesn't work well in the non-linear region of vehicle motion. We are proposing the novel β observer to utilize a_y, the lateral acceleration, together with γ as follows.

$$\begin{aligned}
a_y &= V(\dot{\beta} + \gamma) \\
&= V(a_{11}\beta + a_{12}\gamma + b_1 u + \gamma)
\end{aligned} \tag{14}$$

a_y is represented by (14) and is implemented into the output equation as the form of

$$\dot{\boldsymbol{x}} = \boldsymbol{A}\boldsymbol{x} + \boldsymbol{B}u \tag{15}$$

where

$$\begin{aligned}
\boldsymbol{y} &= \boldsymbol{C}\boldsymbol{x} + \boldsymbol{D}u, \quad \boldsymbol{y} = (\gamma \quad a_y)^T \\
\boldsymbol{C} &= \begin{pmatrix} 0 & 1 \\ V a_{11} & V(a_{12}+1) \end{pmatrix} \\
\boldsymbol{D} &= (0 \quad V b_1)^T
\end{aligned}$$

The observer designed as the full order observer is given by

$$\dot{\hat{\boldsymbol{x}}} = \boldsymbol{A}\hat{\boldsymbol{x}} + \boldsymbol{B}u - \boldsymbol{K}(\hat{\boldsymbol{y}} - \boldsymbol{y}) \tag{16}$$

$$\hat{\boldsymbol{y}} = \boldsymbol{C}\hat{\boldsymbol{x}} + \boldsymbol{D}u \tag{17}$$

The observer poles are assigned to be -200 and $-\frac{C_f+C_r}{MV}$ by adjusting the gain matrix $\boldsymbol{K}$.

Fig.25 is the simulation result of β estimation using the conventional and proposed observers, where we can see the better robustness of the proposed observer.

Here we simulate the situation where we gradually accelerate the vehicle from an initial speed of 20[m/s]. 3[s] later, the steering wheel is turned to give a step input of 3[deg] to the front wheel angle.

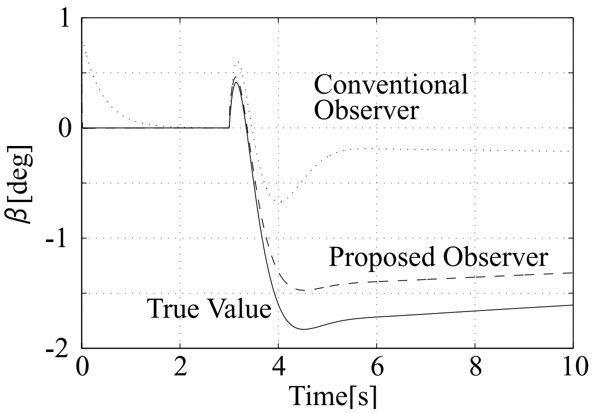

Fig. 25. β estimation using linear observer based on γ and a_y signals.

7 Conclusion

In this paper, I pointed out that EV is the most exciting target of advanced motion control techniques. I introduced our novel experimental EV "UOT March II" completed in 2001. This new four motored EV will play an important role in our novel motion control studies of EV. As the first attempt, we proved the effectiveness of MFC and SRC. The most remarkable point of our research is in utilization of the electric motor's advantage: quick, accurate and distributed torque generation.

Recent concerns on EV is mainly on energy efficiency and environment, but we believe that, in the future, high performance vehicle control must be the major topics, which can be firstly realized by electric vehicles.

We discussed mainly on MFC in this paper, but we have studied on several other motion control issues. For example, Road Condition Estimation, Vehicle Velocity Estimation, Body Slip Angle Estimation, Decoupling of Direct Yaw Moment Control and Active Front Steering, and Hybrid ABS, etc. We plan to carry out experiments on these topics using "UOT March II" and report in the next chance.

8 Acknowledgement

The author would like to state his great appreciation to lots of students in Hori. Lab. and industries for their hard work and kind help in making March I and II and performing various experiments, and also to Mr. T. Okano for his help in editing the manuscript.

References

[1] Ackermann, J., Yaw Disturbance Attenuation by Robust Decoupling of Car Steering, Proc. of 13th IFAC World Congress, 8b-01-1, pp.1-6, 1996.

[2] Daiss, A. and U. Kiencke, Estimation of Tire Slip during Combined Cornering and Braking Observer Supported Fuzzy Estimation, Proc. of 13th IFAC World Congress, 8b-02-2, pp.41-46, 1996.

[3] Furukawa, Y. and M. Abe, Direct Yaw Moment Control with Estimating Side-slip Angle by using On-board-tire-model, Proc. 4th International Symposium on Advanced Vehicle Control (AVEC), pp.431-436, Nagoya, 1998.

[4] Furuya, T., Y. Toyoda and Y. Hori, Implementation of Advanced Adhesion Control for Electric Vehicle, Proc. IEEE Workshop on Advanced Motion Control (AMC), Vol.2, pp.430-4356, 1996.

[5] Gustafsson, F., Slip-based Tire-road Friction Estimation, Automatica, Vol.33, No.6, pp.1087-1099, 1997.

[6] Hori, Y., Y. Toyoda and Y. Tsuruoka, Traction Control of Electric Vehicle based on the Estimation of Road Surface Condition, Basic Experimental Results using the Test EV "UOT March", IEEE Trans. on Ind. Appl., Vol.34, No.5, pp.1131-1138, 1998.

[7] Iwama, N., et. al., Active Control of an Automobile -Independent Rear Wheel Torque Control-, Transactions of SICE, Vol.28, No.27, pp.844-853, 1992.

[8] Liu, C. and H. Peng, Road Friction Coefficient Estimation for Vehicle Path Prediction, Vehicle System Dynamics Supplement, 25, pp.413-425, Swets Zeitlinger, 1996.

[9] Motoyama, S. et. al., Effect of Traction Force Distribution Control on Vehicle Dynamics, Proc. International Symposium on Advanced Vehicle Control (AVEC), No.923080, 1992.

[10] Okano, T, C. Tai, T. Inoue, T. Uchida, S. Sakai and Y. Hori, Vehicle Stability Improvement based on MFC Independently Installed on 4 Wheels -Basic Experiments using "UOT Electric March II"-, Proc. of PCC-Osaka 2002, 2002.

[11] Ray, L. R., Nonlinear Tire Force Estimation and Road Friction Identification: Simulation and Experiments, Automatica, Vol.33, No.10, pp.1819-1833, 1997.

[12] Sado, H., S. Sakai and Y. Hori, Road Condition Estimation for Traction Control in Electric Vehicle, IEEE International Symposium on Industrial Electronics, pp.973-978, Bled, Slovenia, 1999.

[13] Sakai, S., and Y. Hori, Robustified Model Matching Control for Motion Control of Electric Vehicle, Proc. IEEE Workshop on Advanced Motion Control, No.98-025, 1998.

[14] Sakai, S., H. Sado, and Y. Hori, Motion Control in an Electric Vehicle with 4-independently Driven In-wheel Motors, IEEE Trans. on Mechatronics, Vol.4, No.1, pp.9-16, 1999.

[15] Sakai, S., H. Sado, and Y. Hori, Novel Skid Avoidance Method without Vehicle Chassis Speed for Electric Vehicle, Proc. International Power Electronics Conference (IPEC-2000), Vol.4, pp.1979-1984, 2000.

[16] Sakai, S., H. Sado and Y. Hori, Novel Wheel Skid Detection Method for Electric Vehicles, Proc. 16th. Electric Vehicle Symposium (EVS16), pp.75-, Beijing, 1999.

[17] Shibahata, Y. and et. al., The Improvement of Vehicle Maneuverability by Direct Yaw Moment Control, Proc. 1st International Symposium on Advanced Vehicle Control (AVEC), No.923081, 1992.

[18] Sakai, S. and Y. Hori, Advanced Vehicle Motion Control of Electric Vehicle based on the Fast Motor Torque Response, Proc. 5th International Symposium on Advanced Vehicle Control (AVEC), pp.729-736, Michigan, 2000.

[19] Sakai, S, H. Sado, and Y. Hori, Novel Skid Detection Method without Vehicle Chassis Speed for Electric Vehicle, JSAE Review, Vol.21, No.4, pp.503-510, 2000.

[20] Sakai, S., T. Okano, C. Tai, T. Uchida, and Y. Hori, 4 Wheel Motored Vehicle "The UOT March II" -Experimental EV for Novel Motion Control Studies-, Proc. of The First ISA/JEMIMA/SICE Joint Technical Conference, 2001.

[21] Sakai, S., T. Okano, C. Tai, T. Uchida, and Y. Hori, Experimental Studies on Vehicle Motion Stabilization with 4 Wheel Motored EV, Proc. of EVS-18, 2001.

[22] Sul, S. K. and S. J. Lee, An Integral Battery Charger for Four-Wheel Drive Electric Vehicle, IEEE Trans. on Ind. Appl., Vol.31, No.5, 1995.

[23] Wang, Y. and M. Nagai, Integrated Control of Four-Wheel-Steer and Yaw Moment to Improve Dynamic Stability Margin, Proc. 35th IEEE-CDC, pp.1783-1784, 1996.

[24] Yamazaki, S., T. Fujikawa and I. Yamaguchi, A Study on Braking and Driving Properties of Automotive Tires, Transactions of the Society of Automotive Engineers of Japan, Vol.23, No.2, pp.97-102, 1992.

[25] Yamazaki, S., T. Suzuki and I. Yamaguchi, An estimation method of hydroplaning phenomena of tire during traveling on Wet Road, Proc. JSAE Spring Conference No.9932421, pp.5-8, Yokohama, 1999.

Appendix

A How to Implement our Motion Controller into Total Control System

The target of our project is to realize a novel vehicle motion control system with four independently controlled in-wheel motors as depicted in Fig.26

The block named "motion controller" shows the attitude controller to regulate β and γ to realize the desired vehicle characteristics. This part is using week feedback control or basically a feedforward control, which can be realized also in ICV's.

The "dynamic optimal force distributor" generates torque command for each wheel. For example, bigger torque commands are given to tires with smaller side forces, which can be calculated based on the slip angle estimation. δ_r is the rear tire steering angle. Compensation angle to δ_f can be used for the same purpose.

The most important part in Fig.26 is the block "various techniques to improve performance at each wheel". This part plays an essenstial role in our proposal. It requires a fast response which is impossible for IC engine.

Figs.27 and 28 show how MFC and SRC are used as a minor feedback loop in the total vehicle control system. MFC or SRC should be implemented in each wheel as the minor feedback control loop. It helps perfect realization of upper level control strategies, i.e., DYC or VSC.

B Fuel Cell Vehicle -Engine is replaced by Electric Motor

In this Appendix B, I will discuss on configuration of FCV (Fuel Cell Vehicle). There are mainly two ways to understand FCV.

In Fig.29, if we assume Engine is replaced by FC (Fuel Cell)-Stack and Motor, we should compare the engine and FC-Stack in various aspects, e.g., energy efficiency or power/weight ratio. Most people are doing this.

On the other hand, if we assume that Gas Tank is replaced by H2 Tank and FC Stack, Engine is replaced by Motor, and we can compare the engine and the motor in various points. We are standing on this stance.

Which do you think is better? We are pursuing the future possibility of electric motor's advantage to IC engine. FCV uses electric motor. Our development can be utilized into FCV as it is.

Fig.30 shows two ways of calling FCV. If we start from HEV like Toyota Prius, FCHV is the natural name of this vehicle. Its reason is as follows. As FC is not enough in power generation and regenerative braking performance, additional secondary Battery and Motor should be used together. In this meaning, FCV is same to HEV.

On the contrary, if we understand that FCV is just using two types of electric power sources, electric motor plays an important role as the main actuator. In our development in March Project, we do not care about the kinds of energy source. However the usage of electric motor is essential and absolute, because we are utilizing the advantages of electric motor in the viewpoint of control. In this meaning, FCV should not be called FCHV but FCEV.

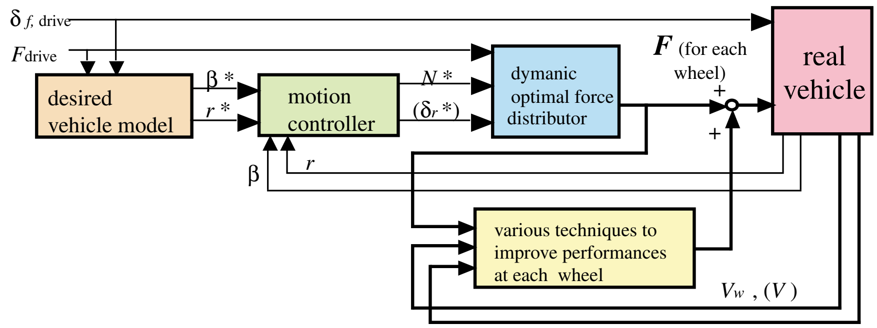

Fig. 26. Whole schematic diagram of the total control system.

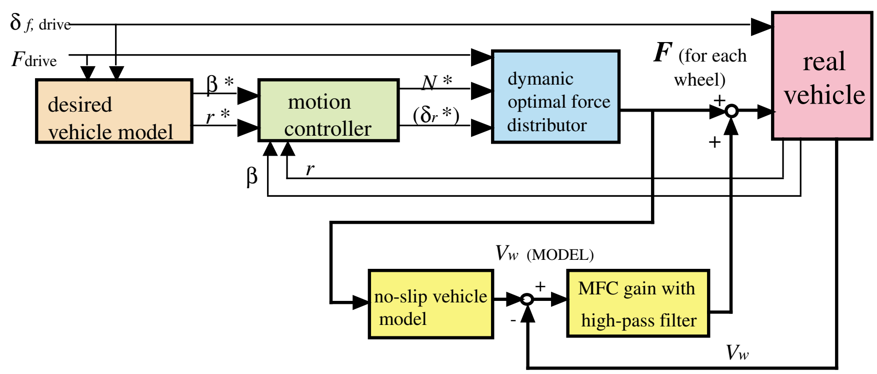

Fig. 27. Implementation of MFC into the whole control system.

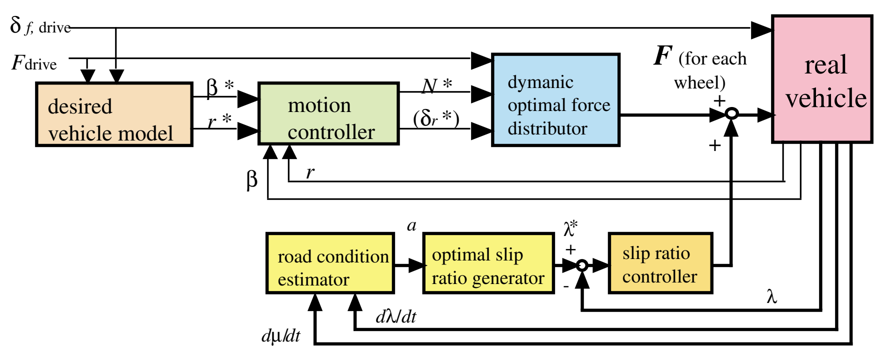

Fig. 28. Implementation of SRC into the whole control system.

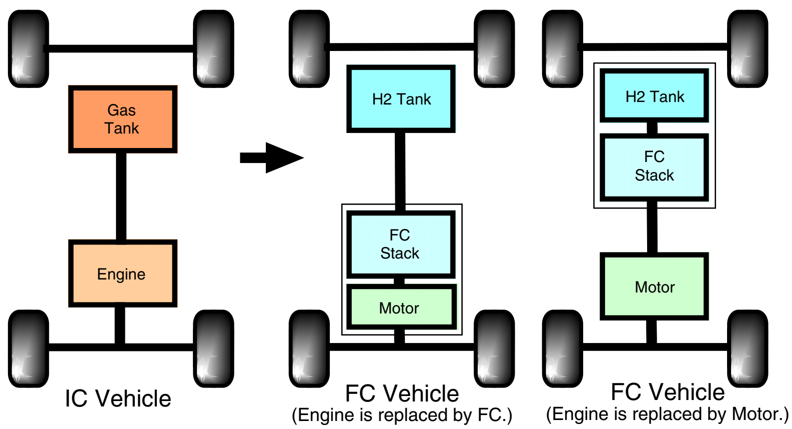

Fig. 29. Two ways to understand FCV.

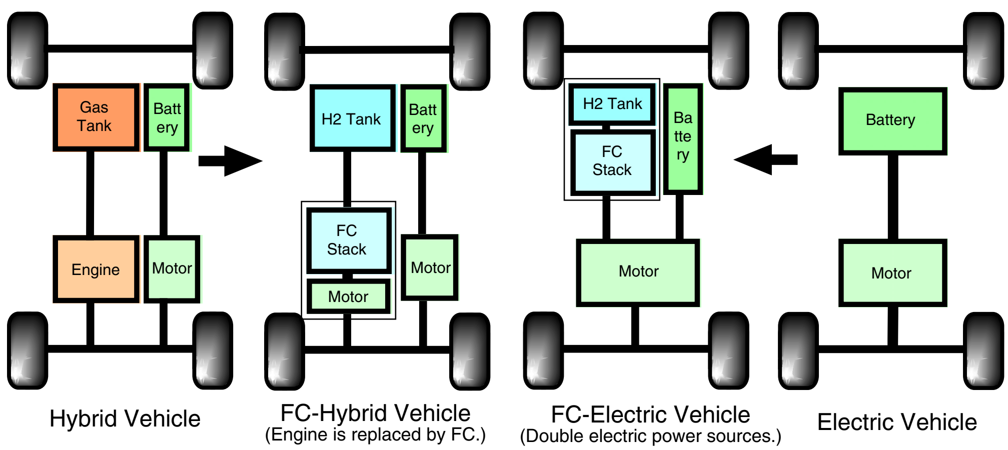

Fig. 30. Two ways to understand FCV with battery, FCHV or FCEV?